

## ULF electromagnetic noise from regional lightning activity: Model and observations

Nadezda V. Yagova<sup>a,\*</sup>, Ashwini K. Sinha<sup>b</sup>, Vyacheslav A. Pilipenko<sup>a</sup>, Evgeny N. Fedorov<sup>a</sup>, Robert Holzworth<sup>c</sup>, Geeta Vichare<sup>b</sup>

<sup>a</sup> The Schmidt Institute of Physics of the Earth of the Russian Academy of Sciences (IPE RAS), B. Gruzinskaya 10, Moscow, Russia

<sup>b</sup> Indian Institute of Geomagnetism, Navi Mumbai, India

<sup>c</sup> University of Washington, Seattle, USA

### ARTICLE INFO

#### Keywords:

ULF waves  
Thunderstorms  
Seismo-electromagnetics

### ABSTRACT

Contribution of lightning to geomagnetic field variations in ULF ( $f < 1$  Hz) frequency range is estimated within the framework of a simple model of ULF response to lightning strokes. ULF lightning index is introduced to quantify a contribution of lightning to ULF power at observational site. The computed pulse series are compared with the pulse-like interference recorded at the low latitude observatory (KNY). Lightning stroke is modeled as a vertical dipole with the perfectly conducting model ionosphere. A program of automatic detection of pulse-like interference in recorded signal is developed. The analysis of the time series of hourly ULF lightning index at KNY during several weeks in summer of 2012 has shown that the contribution of thunderstorms to ULF power may be significant, especially at frequencies  $f > 80$  mHz. This effect should be taken into account in any application utilizing estimates of local ULF power including seismo-electromagnetics.

### 1. Introduction

Measurements of ULF electromagnetic emissions at ground magnetometers are widely used for monitoring the space weather (Guglielmi and Troitskaya, 1974; Pilipenko et al., 1999; Thomas et al., 2015). On the basis of these measurements, various ULF power indices have been suggested, e.g. the Pc5 wave power index in the band 2–7 mHz (Kozyreva et al., 2007), and Pc3 index covering 20–100 mHz band (Heilig et al., 2010). There are attempts to elaborate Pc1 index (0.1 – 1.0 Hz) to characterize the radiation belt electron depletion by ion-cyclotron pulsations (Guglielmi et al., 2006; Miyoshi et al., 2008).

Monitoring of electromagnetic emission at an array of ground stations has become one of the main tools of the electromagnetic earthquake prediction (Hayakawa and Molchanov, 2002; Molchanov and Hayakawa, 2008). Most efforts were concentrated on the ULF and at lower ELF frequencies (from 1 mHz to several tens Hertz), because in this band the attenuation in a conductive crust does not prevent electromagnetic signals originated in the epicenter to reach the ground surface (Hattori, 2004; Schekotov et al., 2007). Quite a few ULF anomalies before large earthquakes were found even with data from relatively low-sensitive flux-gate magnetometers (Hattori, 2004).

A key unresolved problem in these studies is discrimination of weak

seismic-related anomalies from non-seismic disturbances of magnetospheric, ionospheric, atmospheric, or technological origin. Usually, to suppress the influence of magnetospheric pulsations and industrial interference, nighttime intervals are taken for the analysis. Additionally, an influence of magnetospheric ULF pulsations and noise is minimized by selecting days with low geomagnetic activity (Schekotov et al., 2007). To discriminate large-scale ionospheric sources and small-scale disturbances possibly associated with seismic activity, gradient measurements at small baseline was used (Ismaguilov et al., 2003). In the present study, we concentrate on one important feature of ULF observations that is not taken into account in routine ULF data processing - the influence of regional thunderstorms.

Electrical storms are known to be one of the natural sources of electromagnetic emissions in a wide frequency range covering ULF - ELF - VLF - HF bands. The largest spectral density of the atmospheric electrical discharge is concentrated in the VLF band (about several kHz), though essential spectral power is contained in the lower ELF-ULF bands (from fractions of Hz to few tens of Hz). Sporadic local lightning transients and large noise enhancement were observed in the ULF frequency range of several Hz in the thunderstorm proximity (Fraser-Smith, 1993; Fraser-Smith and Kjono, 2014). Lightning strokes are powerful, but not well examined, channel of impact on terrestrial ULF

\* Corresponding author.

E-mail address: [nyagova@ifz.ru](mailto:nyagova@ifz.ru) (N.V. Yagova).

<https://doi.org/10.1016/j.jastp.2018.12.005>

Received 9 April 2018; Received in revised form 20 November 2018; Accepted 14 December 2018

Available online 21 December 2018

1364-6826/ © 2018 Elsevier Ltd. All rights reserved.

electromagnetic field. Dedicated studies showed that evident impulses in the ULF band could be reliably detected by induction magnetometers at distances up to 2000 km from the lightning site (Bösinger et al., 2006). For extreme conditions of the large electric storm, enhancement caused by lightning in the lower ULF frequencies (below 0.1 Hz) was even higher than at higher ULF and ELF frequencies (Fraser-Smith, 1993).

Rather unexpectedly, the influence on ground ULF power of more recently discovered transient light events (TLEs), like red sprites, blue jets, elves, and halos (Fukunishi et al., 1997; Bösinger and Shalimov, 2008), is known in more details than that of ordinary lightning. It may be partly explained by the fact that sprite and halo spectra are enriched by low frequencies and thus a contribution of a single discharge into ULF power is higher. Chang et al. (2014) studied the ULF to VLF amplitude ratio as a sensor for different types of emissions and they found that this ratio for the slowest halo type events exceeds by an order of magnitude as compared to that for elves. Note that in all the cited papers, the authors included Schumann resonance into the ULF frequency range. Lightning contribution to the ULF power in the pulsation frequency range ( $f \leq 1$  Hz) has not been studied in details and we still have not got any effective measure which can give a rough estimate of possible thunderstorm contribution to a recorded ULF power.

In this paper, we suggest an “ULF lightning index” to consider a contribution of lightning discharges to ULF power spectral density. We develop a model of an expected ULF response to local and regional thunderstorms, which might be useful for both the space weather and seismo-forecasting communities.

## 2. Model

A lightning stroke is imagined as a vertical infinitely small electric dipole with current moment  $M_0 = IL$ . An average current associated with lightning is modeled by exponent sum (Nickolaenko and Hayakawa, 2002)

$$\begin{aligned} I(t) &= 0 \quad \text{at } t < 0 \\ I(t) &= \sum_k \exp(-t/t_k) \quad \text{at } t \geq 0 \end{aligned} \quad (1)$$

A power in the ULF band caused by a lightning stroke is determined by current with largest timescale  $t_1$ . Nickolaenko and Hayakawa (2002) give peak currents in 1 from 0.4 to 5 kA at the longest timescale of 7 ms.

Lightning with continuing current are characterized by even longer times. Shindo and Uman (1989) found that the geometric mean duration of long continuing current was 115 ms and the amplitudes ranged from 30 to 200 A. They showed that about 25% negative cloud-to-ground lightning flashes contain a long continuing current.

For the ULF signals, magnetostatic approximation can be used for all the distances where the response to a lightning stroke can be registered. At distances shorter in comparison with the electrosphere height  $h$ , a well-known formula for the magnetic field from a current moment above an infinitely-conductive surface can be used (Greifinger and Greifinger, 1976). At larger distances, an ideally-conducting plane at altitude  $h(f)$ , should be taken into account, where  $h(f)$  is the frequency dependent altitude at which the conduction current becomes equal to the displacement current (Greifinger and Greifinger, 1978). The resultant relationships can be used for an easy evaluation of the expected ground magnetic response at radial distance  $r$  on lightning stroke

$$\begin{aligned} b &= \frac{\mu M_0}{2\pi r^2}, \quad \text{at } r < h \\ b &= \frac{\mu M_0}{2\pi r h}, \quad \text{at } r \geq h \end{aligned} \quad (2)$$

In the further analysis we use the electrosphere height  $h$  and the current moment  $M_0 = IL$ , where  $I$  is the current, and  $L$  is the lightning length as fitting parameters. The dependence of magnetic response on  $h$  is weak, and the best correspondence is found at  $h = 60$  km. Typical amplitudes of  $I$  and  $L$  for continuing current strokes Fan

et al. (2014) give  $10^2 - 3 \cdot 10^3$  A km for  $M_0$ . This gives few nT instantaneous magnetic effect at 10 km distances for  $M_0 = 10^3$  A km, and this result agrees with that of (Ross et al., 2008).

## 3. Observations and data processing

### 3.1. Lightning information

For information about lightning activity, we use the data provided by the global lightning monitoring system WWLLN (Dowden et al., 2002; Rodger et al., 2004). The University of Washington operates this network of lightning location sensors, based on the observations of VLF (3–30 kHz) impulsive signals (“sferics”) from lightning discharges. This network of sferic sensors produces information about timing and location of strokes over the entire globe. The WWLLN network is growing dramatically, its detection efficiency is also rising. Comparative analysis with more dense and expensive commercial networks (Rodger et al., 2004; Abarca et al., 2010) has shown that it detects about  $\sim 10\%$  for all the strokes. The detection efficiency depends on peak current and polarity and it is above 30% for the stroke with peak current  $> 40$  kA. In spite of the chance to detect and locate every lightning stroke is small, the identification efficiency of a thunderstorm center is as high as 90% (Rodger et al., 2006).

### 3.2. Magnetic data and data processing technique

For the analysis, we have used the data of magnetic recording from the Kanoya (KNY) station located in Japan at 31.4°N, 130.9°E. It is equipped with a three-component flux-gate magnetometer with the sampling rate 10 Hz, and the data are available at 1 Hz. The data of 20 months during 2012–2013 for which WWLLN data were also available have been analyzed. The calibration curve is almost flat at  $f < 1$  Hz and the calibration coefficient reaches 1.2 at 5 Hz (Oowada et al., 2003). Although the calibration was done at higher frequencies, as well, the values were not given in (Oowada et al., 2003). Extrapolating, the data in the frequency range 1 – 5 Hz to 10 Hz (100 ms), we can suggest that the 10 Hz signal is reduced by 1.5 – 2 times. As pulses phases are random, not amplitudes but powers of the pulses registered during one sampling are summed and we get for the pulse power from all the lightning

$$b_c^2 = \sum_{k=1}^N b_{ck}^2 \quad (3)$$

where  $c = h, d$  is a component,  $N$  is a number of strokes during a sampling period  $T$ .

Within this calculation scheme, a model “magnetogram” of the impulsive background generated by regional thunderstorms detected by WWLLN is calculated. The resultant impulsive magnetogram is compared with pulse-like interference recorded at the KNY station.

For more effective detection and visualization of pulses in the recorded magnetogram, we use the derivative  $dB/dt$  instead of  $B$ . Pulses with amplitudes above a threshold are selected automatically (the threshold value  $\Delta b_t = 0.1$  nT/s). A pulse recorded in the magnetic response is considered synchronous with one or several strokes, if they are registered within one sampling period. For such pulses, effective distance from a stroke to the observation site is estimated. Then the distance-amplitude dependence is calculated and compared with that predicted by the model dependence given by equation (2).

ULF lightning index is introduced as a ratio of energy of pulses caused by lightning discharges to the ULF energy emitted in a selected frequency range during a given time interval. In the present study, we use hourly lightning index calculated in 0.03–0.24 Hz frequency range. The ULF lightning index is computed using two different approaches. The first one is based on the energy of pulses detected at a station, hereafter called as “observational pulse index”. The second approach

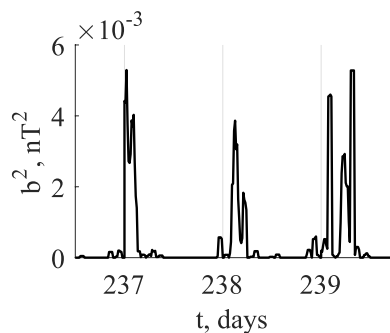


Fig. 1. Diurnal variation of hourly mean energy of a pulse-like ULF interference at KNY during three days in summer of 2012, H component.

utilizes WWLLN lightning data of a pulse sequence and computes the “WWLLN index” based on model calculations.

Other than the thunderstorm activity, industrial interference contributes to pulse-like disturbances. Fortunately, the local industrial interference at KNY has a stable diurnal occurrence. Hourly mean amplitudes of pulse-like signal at KNY for several days in Summer of 2012 are shown in Fig. 1. Stable amplitude variation for all the days leaves no doubts about its industrial origin. It starts at about UT = 20 (LT = 5) and finishes at about UT = 9 (LT = 18). Based on these features, we have chosen 9.5–19 UT night time interval for the analysis of pulse-like interference, which is not influenced by industrial interference.

#### 4. Results of the analysis

##### 4.1. Distance dependence

To illustrate the contribution of regional lightning discharges to ULF recordings, a day with a high thunderstorm activity at Kyushu Island, on June 15, 2012 (day 167) is chosen. Location of lightning registered during this day in the 200 km vicinity of the KNY station are shown in Fig. 2. Total number of lightning discharges recorded by WWLLN in this area exceeds 600. The majority of strokes are grouped into two linear structures elongated in the Southwest-Northeast direction. A histogram illustrating distance distribution between strokes and the observational site is given in Fig. 3. More than 2/3 of lightnings fall into 100 km circle area around KNY.

Fig. 4 shows the measured and modeled time series for the H component of the magnetic field at KNY for a 80 min (4800 points) interval starting at 09:30 UT (the results for D component and total

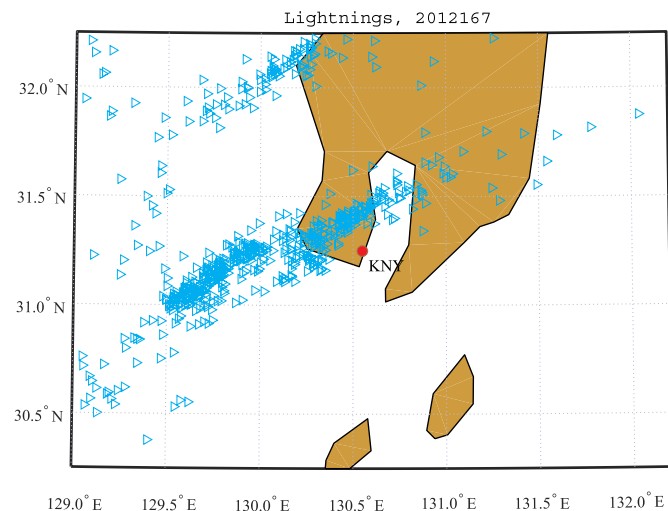


Fig. 2. Lightnings detected at WWLLN near KNY at day 2012167.

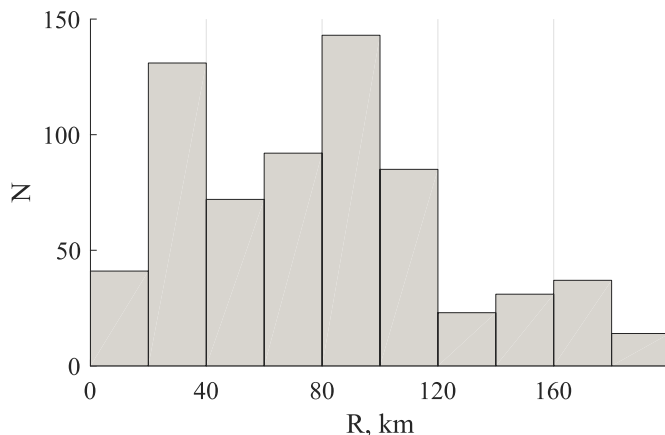


Fig. 3. Distribution of distances between strokes and the observational site.

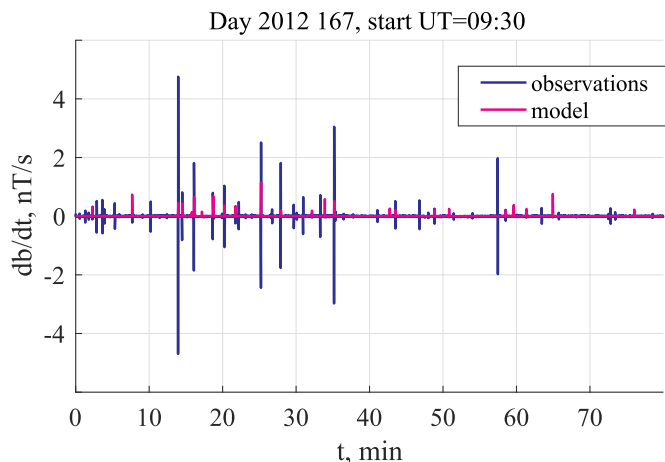


Fig. 4. Recorded and modeled variations of the magnetic field at KNY.

horizontal power are almost identical and they are not shown). During this time interval, the total number of pulses with amplitudes exceeding the threshold is  $L_1 = 37$ . Good synchronization of the majority of pulses is in favor of their thunderstorm origin. Under the threshold value 2 nT/s, the number of pulses registered at KNY simultaneously with WWLLN pulses is  $L_{12} = 9$ . According to WWLLN database the total number of pulses is  $L_2 = 21$ . Note, that random coincidence gives  $P_R = P_1 P_2 \leq 4 \cdot 10^{-5}$ , where  $P_1 = L_1/L$  and  $P_2 = L_2/L$ , i.e.  $P = L_{12}/L = 2 \cdot 10^{-3} \gg P_R$ . The 10% detection rate for individual lightning strokes, reported for WWLLN, results in the pulses registered at KNY without a corresponding stroke in WWLLN database. The strokes which give no response in ULF may be interpreted as a stroke without a continuing current.

We use the distance dependence of pulse amplitude for both registered and WWLLN pulses for model verification. The dependence of the pulse amplitudes on the distance  $R$  between the KNY station and the stroke is given in Fig. 5. Model pulse amplitudes agree with measured ones at distances between 10 and 100 km. At shorter distances, model to measured amplitude ratio grows, probably, because of artificial suppression of high amplitude peaks in magnetic recordings or saturation of data acquisition system and a deviation from theoretical dependence for a point dipole.

The oversimplified model of a single discharge and the propagation media (1–2) gives the best correspondence to measured pulse amplitudes for the current moment  $M_0 = 1500$  A km. This result does not take into account the dependence of calibration constant on frequency. It grows to 2000 – 3000 A km if the calibration coefficient lies between 1.5 and 2, as follows from the extrapolation of data given in (Oowada

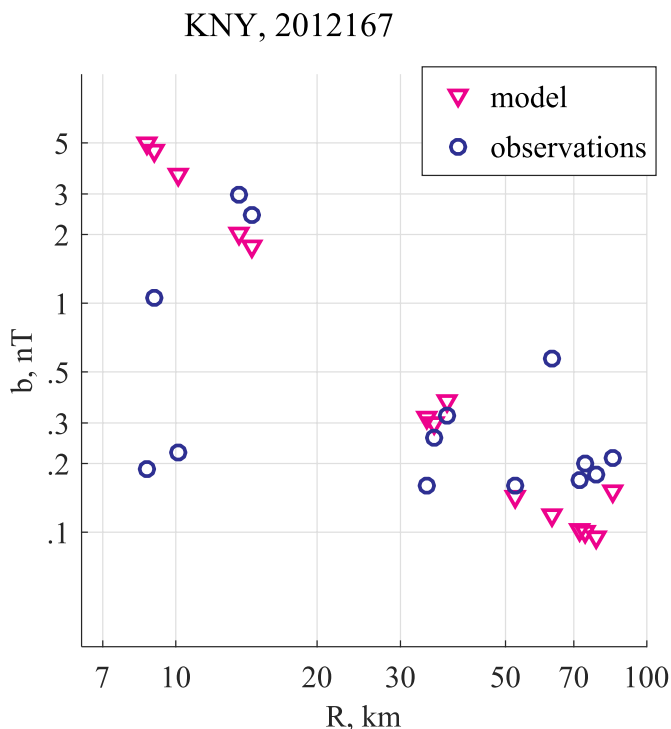


Fig. 5. Dependence of measured at KNY and model pulse amplitude on the effective distance  $R$ .

et al., 2003). These values lie near the upper boundary of the  $M_0$  range for registered lightning strokes with continuing currents.

#### 4.2. Lightning contribution to ULF power

To estimate the average contribution of regional thunderstorm activity to ULF spectral power in Pc2 and Pc3 frequency bands, we use local night hours during summer period of the year 2012 with a noticeable thunderstorm activity near KNY (days 151–250). We compare hourly mean total horizontal power of pulses modeled from WWLLN data and detected from KNY recordings. The time series of ULF lightning index are given in Fig. 6. The modeled WWLLN index and the “observational pulse index” are given in magenta and blue, respectively. The background values of  $W_L$  do not exceed 0.01, while its peak values are about several tenths and the maximal modeled  $W_L \approx 1$ . The correlation between the power logarithms time series (for the non-zero intervals) is  $C = 0.45$ .

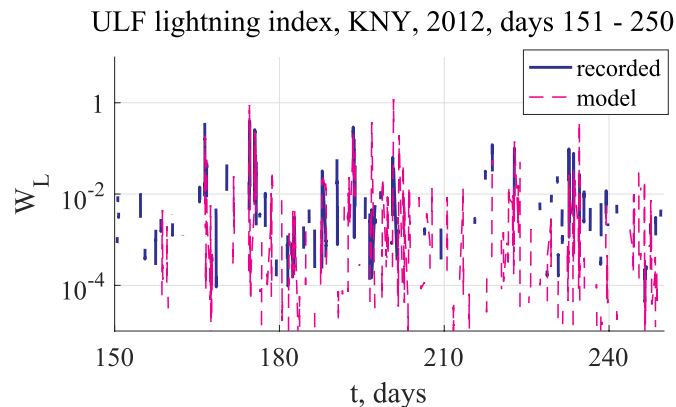


Fig. 6. Modeled and recorded values of hourly ULF lightning index at KNY for nighttime in summer of 2012.

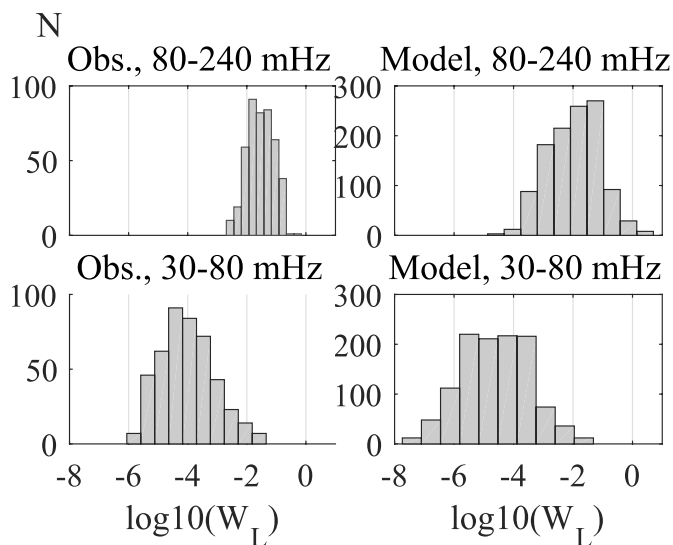


Fig. 7. The distributions of the “observational pulse index” and for the WWLLN lightning index for the nominal Pc3 (30–80 mHz) and Pc2 (80–240 mHz) frequency ranges.

#### 4.3. Statistical relationships

Averaged power spectral density (PSD) in the ULF frequency range decreases with frequency as  $f^{-\alpha}$  (Surkan and Lanzerotti, 1974; Lanzerotti et al., 1990) where  $\alpha$  can vary from 1 to 4 at different latitudes. Hence, lightning contribution to ULF power must grow with frequency. This effect is illustrated in Fig. 7 for both “modeled WWLLN lightning index” and “observational pulse index”. Histograms of decimal logarithms of both modeled and observational indices calculated for all the intervals when the particular index is non-zero, are given at the lower/upper panels for the nominal Pc3 (30–80 mHz) and Pc2 (80–240 mHz) frequency ranges. The distributions of the “observational pulse index” and the WWLLN lightning index are given at left/right panels, respectively. Both observational and model indexes are essentially higher in the Pc2 frequency range. In the Pc3 range pulse contribution to total spectral power does not exceed 0.1, whereas for the Pc2 range maximal index values approach unity. Thus the contribution of regional thunderstorms in high thunderstorm season cannot be ignored.

### 5. Discussion

Lightning activity contribution to ULF electromagnetic disturbances remains the least explored aspect in the lithosphere - atmosphere - ionosphere coupling (Pilipenko, 2012), despite several attempts to examine a significance of thunderstorm activity. Izutsu (2007) estimated the influence of lightning on pulse observing system by investigating which lightning is recorded. Since the numbers for recorded lightning is far greater than the number of pulses recorded, it may be assumed that system records only stronger lightning noise. They focused on how far lightning affects the observation system. A simple parameter  $T \approx I/R$ , where  $I$  is the average lightning current,  $R$  is the distance of the observational site from the stroke was introduced for evaluating the importance of each lightning. This parameter plays the same role as the ULF-lightning index, suggested in this paper.

Our analysis with an oversimplified model and the data recorded by the flux-gate magnetometer has shown that thunderstorm activity contributes essentially to ULF power at distances up to few hundred kilometers from the observational point. Case as well as statistical studies using search coil magnetometer data from Japanese station MSR (Schekotov et al., 2011) clearly demonstrated the lightning contribution to the ULF power in the Ionospheric Alfvén Resonator (IAR)

frequency range at distances up to several hundred kilometers. Moreover, local thunderstorm may play a role of an energy source for IAR (Fedorov et al., 2006; Surkov et al., 2006). For these frequencies, an analysis of magnetic field from a lightning discharge should include a realistic model of the ionosphere. Such a consideration based on the International Reference Ionosphere model (IRI) is given by Fedorov et al. (2016). Due to mode conversion and resonant effects, frequency and distance dependence of magnetic field becomes non-monotonic. However, these effects are essential at higher frequencies and distances from the source, than in the present study, while at low frequencies and short distances, the dependence of  $b_{\varphi}$  component on distance is close to a simple model (2).

In the opposite case of short distances from a stroke ( $R \simeq L$ ), the approximation of a point source is not valid. This leads to a severe disagreement of modeled and measured distance dependencies of pulse amplitude, seen in Fig. 5.

The problem of the absence of the one-to-one correspondence between ULF pulses and WWLLN lightning can be divided into two sub-problems: lightning without ULF counterpart and vice-versa. The ULF peaks with no corresponding lightning may be attributed to the limited sensitivity of WWLLN network, while the lightning discharges with no ULF correspondence may be the result of lower ULF response to negative strokes with a weaker low frequency tail (see e. g. Bösinger and Shalimov (2008); Shalimov and Bösinger (2008) and references therein).

The distances, where thunderstorm activity should be taken into account in the analysis of ULF signals, depends essentially both on magnetometer sensitivity and time averaging. The ULF lightning index suggested here is aimed on continuous monitoring at networks equipped with fluxgate magnetometers, like INTERMAGNET, and it uses data with time averaging from 10 min to 1 h. This leads to relatively short distances where the thunderstorm effect is not only detectable in time domain, but provides a non-negligible contribution to the spectral power in the Pc2-3 frequency range.

The above analysis shows, that regional thunderstorms contribute to ULF power, especially at  $f > 80$  mHz. It can be a source of false alarms in ULF power if a thunderstorm occurs before an earthquake. Generally, a false alarm in seismo-electromagnetic problems can arise either due to genuine physical reason, or it can be an artifacts of data processing. Although pulse-like interference can be easily seen in the magnetogram, all the information, other than amplitude, may be lost in spectral representation. Fedorov et al. (2014) have discussed the reasons of false interpretation of spectral information if it was used without waveforms. This difficulty can be overcome, if special algorithms aimed on automatic detection of pulses are applied.

Contribution of regional thunderstorms to ULF spectral power can lead to false correlations and wrong interpretation of local variations of ULF parameters as seismo-electromagnetic effects because of two common features of spatial distributions of thunderstorms and

variations of parameters of natural ULF noise, probably related to seismicity:

- Spatial scales of both zones, the first of reported electromagnetic precursors in the ULF frequency range (see e.g. Molchanov and Hayakawa (2008) and references therein), and the second of a non-negligible contribution of thunderstorms to ULF power are about several hundred kilometers.
- Fronts of thunderstorms often reproduce the isolines of relief, and at least some of reported electromagnetic precursors are oriented along active faults.

The second feature follows naturally from the fact, that tectonic faults and mountain ranges in many regions are approximately parallel to each other, and that relief irregularities influence thunderstorm activity via rainfall. As a result, zones of maximal thunderstorm intensity tend to repeat the geometry of faults. Fig. 8(a) depicts an example of such a distribution of lightnings, registered on Day 2012 155. The lightnings form a line, nearly parallel to the fault (yellow line) and the sea shore. However, such a distribution of lightnings does not exist permanently. Fig. 8(b) shows a distribution of lightnings in the same region a week before (Day, 2012 148). On this day, lightnings form two lines, the first dense line goes along a sea shore, and the second with lower density of lightnings, crosses the fault. It follows from our analysis of thunderstorm contribution to ULF power, that such change of spatial distribution of lightnings should result in variation of amplitude of natural ULF noise in this region. If this change of spatial distribution of lightnings coincides in time with seismic activation, it can be wrongly interpreted as a seismo-electromagnetic effect. This means that regional thunderstorm activity and controlling meteorological factors should be taken into account in seismo-electromagnetic studies, to avoid false correlations.

## 6. Conclusion

We have used a simple model to estimate lightning contribution to the geomagnetic field in the ULF ( $f < 1$  Hz) frequency range. An individual lightning is modeled by a vertical dipole located between the two ideally conducting surfaces: the Earth and the ionosphere. Pulse amplitude in the ULF frequency band is estimated from the continuing current with typical timescales 10 – 100 ms. To verify the model, a program of automatic detection of pulse-like interference in recorded signal is developed and applied to the geomagnetic field variations at the KNY station.

The ULF lightning index has been introduced as a PSD ratio of pulses associated with lightning to total PSD in a given frequency range. Two variants of this index have been suggested. Within the first approach, we have calculated the “modeled WWLLN lightning index” based on the power of pulse series generated by lightning in the vicinity

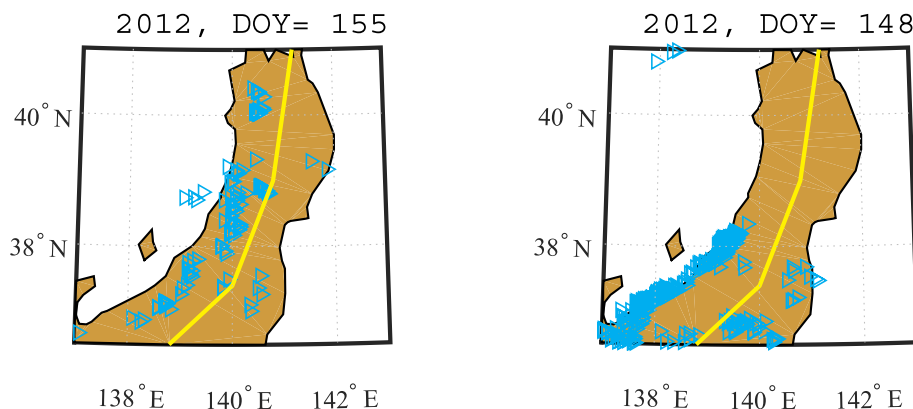


Fig. 8. An example of change of spatial distribution of lightnings in Honsyu region: (a) Day 2012 155; (b) day 2012 148.

of the observation site. Lightning locations and timings are taken from WWLLN data, while the ULF response to a lightning discharge is estimated within the framework of developed model. Within the second approach, we have calculated the “observational pulse index”. It is based on the automatic detection of pulse-like interference in the recorded signal during the night hours, when the industrial interference is low. The parameters of the model dipole are selected from the fitting distance dependence of recorded and modeled pulse amplitude and the correlation between modeled and measured ULF indices.

Our analysis has shown that both, modeled and measured hourly ULF lightning indices vary in correlated way, and their absolute values demonstrate a suitable agreement in Pc3 (20–80 mHz) and Pc2 (80–240 mHz) frequency bands. The average contribution of lightning to ULF power estimated at the KNY station with a 1-h ULF lightning index is about  $10^{-4}$  and  $3 \cdot 10^{-2}$  in the Pc3 and Pc2 frequency ranges, respectively. On the contrary, both indexes calculated for the time intervals with nearby thunderstorms reach 0.1/1 in the Pc3/Pc2 frequency ranges. Thus, the contribution of thunderstorms to ULF power at timescales of about or shorter than 1 hr may be significant, and it should be taken into account, at least in the form of ULF lightning index in any application based on local ULF power including seismo-electromagnetics.

### Acknowledgement

The data of KNY observatory operated by the Kakioka Magnetic Observatory of the Japan Meteorological Agency (<http://www.kakioka-jma.go.jp/en/>) are provided by the World Data Center for Geomagnetism, Kyoto (<http://wdc.kugi.kyoto-u.ac.jp/index.html>). The work of NY, EF, and VP is supported by the RFBR grant No. 18-05-00108A.

### Appendix A. Supplementary data

Supplementary data to this article can be found online at <https://doi.org/10.1016/j.jastp.2018.12.005>.

### References

- Abarca, S.F., Corbosiero, K.L., Galarneau Jr., T.J., 2010. An evaluation of the worldwide lightning location network (WWLLN) using the national lightning detection network (NLDN) as ground truth. *J. Geophys. Res.* 115, D18206. <https://doi.org/10.1029/2009JD013411>.
- Bösinger, T., Mika, A., Shalimov, S.L., Haldoupis, C., Neubert, T., 2006. Is there a unique signature in the ULF response to sprite-associated lightning flashes? *J. Geophys. Res.* 111, A10310. <https://doi.org/10.1029/2006JA011887>.
- Bösinger, T., Shalimov, S.L., 2008. On ULF signatures of lightning discharges. *Space Sci. Rev.* 137, 521532. <https://doi.org/10.1007/s11214-008-9333-4>.
- Chang, S.-C., Hsu, R.-R., Huang, S.-M., Su, H.-T., Kuo, C.-L., Chou, J.-K., Lee, L.-J., Wu, Y.-J., Chen, A.B., 2014. Characteristics of TLE-producing lightning in a coastal thunderstorm. *J. Geophys. Res. Space Phys.* 119, 9303–9320.
- Dowden, R.L., Brundell, J.B., Rodger, C.J., 2002. VLF lightning location by time of group arrival (TOGA) at multiple sites. *J. Atmos. Sol. Terr. Phys.* 64, 817–830.
- Fan, X., Zhang, G., Wang, Y., Li, Y., Zhang, T., Wu, B., 2014. Analyzing the transmission structures of long continuing current processes from negative ground flashes on the Qinghai-Tibetan Plateau. *J. Geophys. Res. Atmos.* 119, 20502063. <https://doi.org/10.1002/2013JD020402>.
- Fedorov, E., Schekotov, A. Ju, Molchanov, O.A., Hayakawa, M., Surkov, V.V., Gladichev, V.A., 2006. An energy source for the mid-latitude IAR: World thunderstorm centers, nearby discharges or neutral wind fluctuations? *Phys. Chem. Earth, Parts A/B/C* 31, 462–468.
- Fedorov, E., Schekotov, A., Hobar, Y., Nakamura, R., Yagova, N., Hayakawa, M., 2014. The origin of spectral resonance structures of the ionospheric Alfvén resonator. Single high-altitude re-reflection or resonant cavity excitation? *J. Geophys. Res. Space Phys.* 119, 3117–3129. <https://doi.org/10.1002/2013JA019428>.
- Fedorov, E., Mazur, N., Pilipenko, V., Baddeley, L., 2016. Modeling the high-latitude ground response to the excitation of the ionospheric MHD modes by atmospheric electric discharge. *J. Geophys. Res. Space Phys.* 121 (11). <https://doi.org/10.1002/2016JA023354>. 28211,301.
- Fraser-Smith, A.C., 1993. ULF magnetic fields generated by electrical storms and their significance to geomagnetic pulsation generation. *Geophys. Res. Lett.* 20, 467–470.
- Fraser-Smith, A.C., Kiono, S.N., 2014. The ULF magnetic fields generated by thunderstorms: a source of ULF geomagnetic pulsations? *Radio Sci.* 49, 1162–1170.
- Fukunishi, H., Takahashi, Y., Sato, M., Shono, A., Fujito, M., Watanabe, Y., 1997. Ground-based observations of ULF transients excited by strong lightning discharges producing elves and sprites. *Geophys. Res. Lett.* 24, 2973–2976.
- Greifinger, C., Greifinger, P., 1976. Transient ULF electric and magnetic fields following a lightning discharge. *J. Geophys. Res.* 81, 2237–2247.
- Greifinger, C., Greifinger, P., 1978. Approximate method for determining ELF eigenvalues in the earth-ionosphere waveguide. *Radio Sci.* 13, 831–837.
- Guglielmi, A.V., Troitskaya, V.A., 1974. Diagnostics of the magnetosphere and interplanetary medium by means of pulsations. *Space Sci. Rev.* 16, 331–345.
- Guglielmi, A., Potapov, A., Matveyeva, E., Polyushkina, T., Kangas, J., 2006. Temporal and spatial characteristics of Pc1 geomagnetic pulsations. *Adv. Space Res.* 38, 1572–1575.
- Hattori, K., 2004. ULF geomagnetic changes associated with large earthquakes. *Terr. Atmos. Ocean Sci.* 15, 329–360.
- Hayakawa, M., Molchanov, O. (Eds.), 2002. *Seismo Electromagnetics, Lithosphere-atmosphere-ionosphere Coupling*. TERRAPUB, Tokyo, pp. 477.
- Heilig, B., Lotz, S., Veró, J., Sutcliffe, P., Reda, J., Pajunpää, K., Raita, T., 2010. Empirically modeled Pc3 activity based on solar wind parameters. *Ann. Geophys.* 28, 1703–1722.
- Ismagilov, V.S., Kopytenko, Yu A., Hattori, K., Hayakawa, M., 2003. Variations of phase velocity and gradient values of ULF geomagnetic disturbances connected with the Izu strong earthquakes. *Nat. Hazards Earth Syst. Sci.* 3, 211–215.
- Izutsu, J., 2007. Influence of lightning on the observation of seismic electromagnetic wave anomalies. *Terr. Atmos. Ocean Sci.* 18, 923–950.
- Kozyreva, O., Pilipenko, V., Engebretson, M.J., Yumoto, K., Watermann, J., Romanova, N., 2007. In search of a new ULF wave index: comparison of Pc5 power with dynamics of geostationary relativistic electrons. *Planet. Space Sci.* 55, 755–769.
- Lanzerotti, L.J., MacLennan, C.G., Fraser-Smith, A.C., 1990. Background magnetic spectra from  $10^0$  to  $10^5$  Hz. *Geophys. Res. Lett.* 17, 1593–1596.
- Miyoshi, Y., Sakaguchi, K., Shiokawa, K., Evans, D., Albert, J., Connors, M., Jordanova, V., 2008. Precipitation of radiation belt electrons by EMIC waves, observed from ground and space. *Geophys. Res. Lett.* 35, L23101. <https://doi.org/10.1029/2008GL035727>.
- Molchanov, O., Hayakawa, M., 2008. *Seismo Electromagnetics and Related Phenomena: History and Latest Results*. TERRAPUB, Tokyo, pp. 189.
- Nickolaenko, A.P., Hayakawa, M., 2002. Resonances in the Earth-ionosphere cavity. Kluwer Academic Publisher - Dordrecht/Bosyon/London, pp. 392.
- Oowada, T., Tokumoto, T., Yamada, Y., Ozima, M., Kumasaka, N., Yokoyama, M., Sugawara, M., Koike, K., Shimizu, Y., 2003. *Introduction to Our New System: Magnetometer for Wide Frequency Range, vol. 1. Technical Report of the Kakioka Magnetic Observatory, Selected Translations*, pp. 1–48.
- Pilipenko, V., Yumoto, K., Fedorov, E., Yagova, N., 1999. Hydromagnetic spectroscopy of the magnetosphere with Pc3 geomagnetic pulsations at 210 meridian. *Ann. Geophys.* 17, 53–65.
- Pilipenko, V.A., 2012. Impulsive coupling between the atmosphere and ionosphere/magnetosphere. *Space Sci. Rev.* 168, 533–550.
- Rodger, C.J., Brundell, J.B., Dowden, R.L., Thomson, N.R., 2004. Location accuracy of long distance VLF lightning location network. *Ann. Geophys.* 22, 747–758. <https://doi.org/10.5194/angeo-22-747-2004>.
- Rodger, C.J., Werner, S., Brundell, J.B., Lay, E.H., Thomson, N.R., Holzworth, R.H., Dowden, R.L., 2006. Detection efficiency of the VLF world-wide lightning location network (WWLLN): initial case study. *Ann. Geophys.* 24, 3197–3214.
- Ross, M., Cummer, S.A., Nielsen, T.K., Zhang, Y., 2008. Simultaneous remote electric and magnetic field measurements of lightning continuing currents. *J. Geophys. Res.* 113, D20125. <https://doi.org/10.1029/2008JD010294>.
- Shalimov, S., Bösinger, T., 2008. On distant excitation of the ionospheric Alfvén resonator by positive cloud-to-ground lightning discharges. *J. Geophys. Res.* 113, A02303. <https://doi.org/10.1029/2007JA012614>.
- Shindo, T., Uman, M.A., 1989. Continuing current in negative cloud-to-ground lightning. *J. Geophys. Res.* 94 (D4), 5189–5198.
- Schekotov, A.Y., Molchanov, O.A., Hayakawa, M., Fedorov, E.N., Chebrov, V.N., Sinitin, V.I., Gordeev, E.E., Belyaev, G.G., Yagova, N.V., 2007. ULF/ELF magnetic field variations from atmosphere induced by seismicity. *Radio Sci.* 42, RS6S90. <https://doi.org/10.1029/2005RS003441>.
- Schekotov, A., Pilipenko, V., Shiokawa, K., Fedorov, E., 2011. ULF impulsive magnetic response at mid-latitudes to lightning activity. *Earth Planets Space* 63, 119–128.
- Surkan, A.J., Lanzerotti, L.J., 1974. ULF geomagnetic power near  $L = 4.3$ . Statistical study of power spectra in conjugate areas during December solstice. *J. Geophys. Res.* 79, 2403–2412. <https://doi.org/10.1029/JA079i016p02403>.
- Surkov, V.V., Hayakawa, M., Schekotov, A.Y., Fedorov, E.N., Molchanov, O.A., 2006. Ionospheric Alfvén resonator excitation due to nearby thunderstorms. *J. Geophys. Res.* 111, A01303. <https://doi.org/10.1029/2005JA011320>.
- Thomas, N., Vichare, G., Sinha, A.K., Rawat, R., 2015. Low-latitude Pi2 oscillations observed by polar low earth orbiting satellite. *J. Geophys. Res. Space Phys.* 120, 7838–7856.